

# Fundamental Study on End Resistance of Bored Precast Pile

*Toshihide Yamashita*

Maeda Co., Ltd., Chiyoda, Tokyo, Japan

*Hideto Sato*

Department of Architecture & Life Design, Nihon University Junior College, Funabashi, Chiba, Japan

*Yutaka Kubo and Keizo Minagawa*

System Keisoku Co., Ltd., Sumida, Tokyo, Japan

*Katsuhiko Kanuka*

Kanuka Design Co., Ltd, Yokohama, Kanagawa, Japan

## ABSTRACT

In the bored precast pile construction method, precast concrete pile or steel pipe pile is used, and small sized piles also apply to this method.

The objective of this study is to develop an effective pile end shape for a small-diameter steel pipe pile, which can work even if the stiffness of the cement paste around the pile tip would be insufficient. Laboratory experiment for static axial compressive load test of single pile in which the tip was covered with plaster was performed. The end resistance was larger than that of a bared pile, but when the displacement progressed, the resistance decreased because of destruction of the root part. The behavior of the end resistance and relationship of the strength of the root part were discussed, and a simplified calculation method was proposed.

**KEY WORDS:** Bored precast pile; end bearing capacity; laboratory experiment; simplified analysis.

## INTRODUCTION

The bored precast pile method is a major pile construction method in Japan. The application number of this method is increasing in urban areas because of less noise and low vibration. Recently, small sized piles also apply to this method for small building's foundations such as detached residences or retaining walls.

It is necessary to build a homogeneous and strong root solidifying part in the pile end zone. The root part is designed to have sufficient strength, and is managed as strictly as possible. However, the strength of the root part may be insufficient due to the unevenness and dispersion of the ground layer, and some errors of the control of the installation. If the pile end is fixed to a hard layer, such as dense sand or gravel layer, the sufficient end resistance can be obtained because it is relatively easy to

build the root hardening part with good quality. However, in the case of a soft cohesive layer or saturated medium sandy layer, the end resistance can be short. It is surmised that the cause of this phenomenon is destruction of the root part, and it occurs due to weakness of the root part and/or insufficient stiffness of the soil around the pile end.

Some destruction patterns in the root hardening part have been observed in previous research. Ueno and Kurachi (1993) reported compressive destruction and punching destruction as typical patterns. Kiya and Kato (2007) pointed out a thin root hardening part can be the cause of the punching destruction, while a thick case can cause cleavage destruction. On the other hand, Ishikawa and Ito (2012) stated the destructive form of the root part is affected by the thickness and the strength of the root. Tsuchiya and Kuwabara (2012) reported the strength of the root part is determined mainly by the effective cement-water ratio which considers the water content in the original ground. Miyazaki and Sato (2015) and Sato and Kanuka (2016a) indicated that the end disk plate attached to the pile tip is effective to exhibit good performance of the end bearing capacity for a small-diameter steel pipe pile. Furthermore, Sato and Kanuka (2016b) reported that un-hardened root could not transmit the stress from the pile body to the ground below by the visualization experiments.

The objective of this study is to make clear the characters of the end resistance for the bored precast pile with the weak root part. The authors performed small sized model tests of static axial compressive loading for single piles. Air dry silica sand was used for model ground. The test pile of which tip was covered with plaster was set up simulating actual stress condition of the prebored pile construction method in the pile end area. We discuss the end resistance and destruction pattern of the root part. Then, we try to propose a simplified calculation method that can estimate the end resistance of bored precast pile in consideration of the destruction of the root hardening part.

## VERTICAL LOADING TEST

### Test Piles and Test Series

A steel pipe, 48.6 mm in diameter ( $D$ ) and 3.2 mm in thickness ( $t$ ), was used as test pile. The length of the pile is 600 mm and the pile ends were covered with plaster in order to imitate root hardening parts with insufficient stiffness.

Figs. 1, 2 and table 1 show the test pile shapes and details. A steel pipe with a steel disk (48.6 mm in diameter) attached at the tip is used as a closed end pile (SP). In this paper, the SP is not covered with plaster and is treated as the standard pile. The embedment length ( $H$ ) of SP is 243 mm (5D). A test series of C, from CPT-60 to CPT-120 are performed to

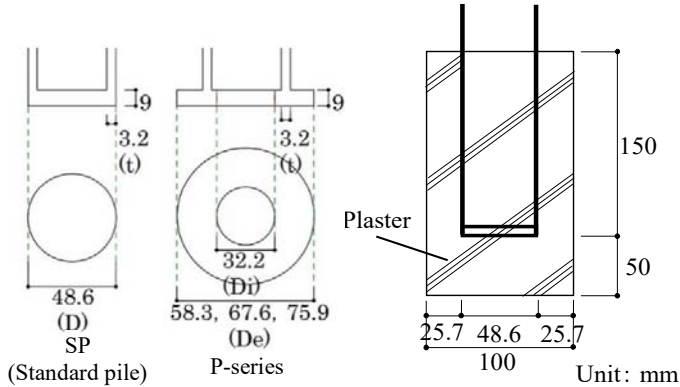


Fig. 1 End shape of test pile

Fig. 2 Detail of root part (C-series)

Table 1 Test pile Factors

Series	Symbol	Water-Plaster Ratio $W/P$ (%)	External diameter of pile end $D_e$ (mm)	Pile end diameter $D$ (mm)
-	SP(Standard)	-	48.6	48.6
C-series	C-60	60	48.6	100
	C-80	80		
	C-100	100		
	C-120	120		
P-series	P-58	120	58.3	100
	P-68		67.6	
	P-75		75.9	

Table 2 Model ground characteristics

Sand	Silica sand (No.5)
Method	Air-pluviation
Density ( $\rho$ )	1760 kg/m <sup>3</sup>
Void ratio ( $e$ )	0.512
Relative density ( $D_r$ )	87.50 %
Internal friction angle ( $\phi$ )	45°

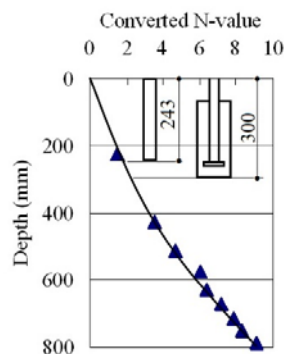


Fig. 3 Distribution of N-values

investigate the influence of the root strength. The pile ends are covered with plaster in which water-plaster ratios ( $W/P$ ) are 60% to 120%. The diameter of the root part is 100 mm and the thickness of the plaster is 50 mm. The embedment length ( $H$ ) of C-series is 300 mm.

A test series of P is carried out to discuss the effect of end disk plate. At the pile tips of the P-series, holed disks with an opening diameter ( $D_i$ ) of 32.2 mm and an external diameter ( $D_e$ ) of 58.3, 67.6 and 75.9 mm are fixed to the pile tips. The pile ends are also covered with plaster of which  $W/P$  is 120 %. The dimensions of the root part are the same as C-series, and the embedment length is also 300 mm.

### Model Ground Preparation

A steel circular test tank with a diameter of 1,000 mm and a depth of 1,000 mm is used. No. 5 silica sand in dry condition is used for the model ground. The test ground is prepared by the air-pluviation technique with double nets for dispersion. The characteristics of the model ground are shown in table 2.

In order to produce pile tip peripheral ground conditions approximate to the bored pile construction method, model ground preparation and setting up of the test pile is executed as follows.

1. The model ground is built up to the bottom of the root part.
2. The test pile covered by plaster is placed in the center of the tank.
3. The test tank is filled to the rim.

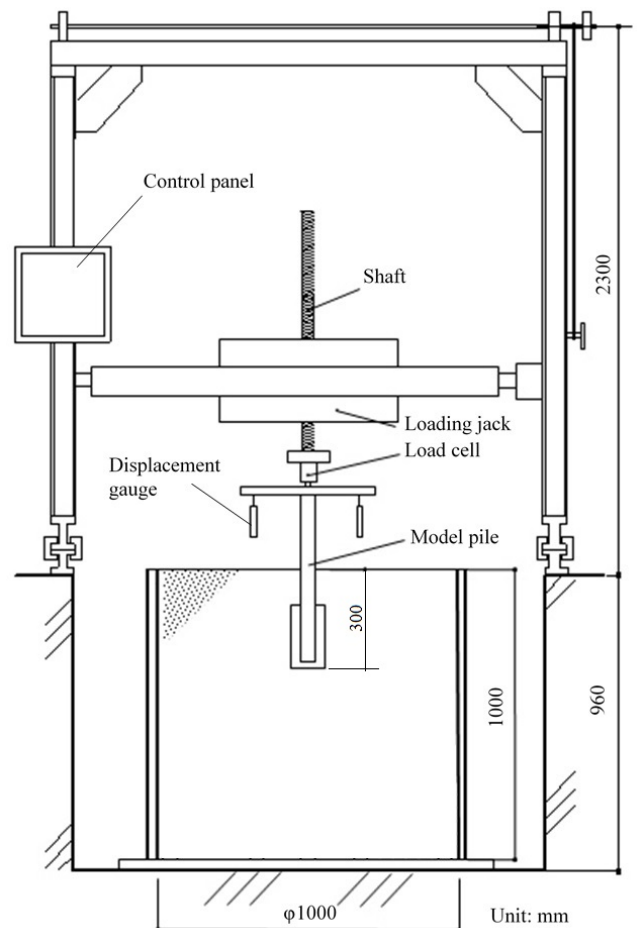


Fig. 4 Experimental apparatus

Fig. 3 shows the distribution of the converted N-values of SPT (standard penetration test). The converted N-value is obtained by dividing the specified penetration length of the SPT (300 mm) by the penetration length of one drop. From fig. 3, the N-value of the pile end ( $N_i$ ) is estimated.

### Loading and Measurement Method

For axial loading test, a displacement controlling type loading device is used (see fig. 4), and the loading speed is 0.1 mm/min. The pile head load and displacement are measured in intervals of 3 seconds by load cell and two displacement gages.

In this laboratory experiment, the resistance and the displacement of the pile end are almost equal to the values of the pile head, because the pile length is relatively short and frictional resistance of the pile surface is exceedingly small. Accordingly, in this paper, the pile head load and pilehead displacement are estimated as the pile end resistance and the pile end displacement, respectively.

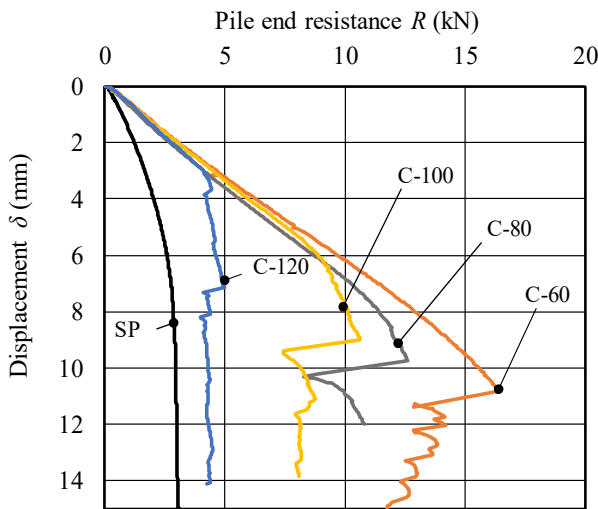


Fig. 5 Relationship between displacement and pile end resistance (C-series)

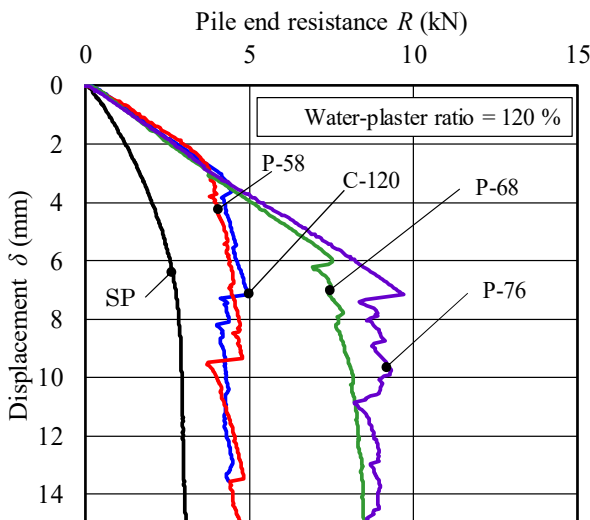


Fig. 6 Relationship between displacement and pile end resistance (P-series)

## RESULTS OF LABORATORY EXPERIMENT

Figs. 5 to 6 shows the test results of the show the results of the C-series and P-series, the relationships between the pile end resistance ( $R$ ) and displacement of pile ( $\delta$ ), and the test pile without root part (SP: standard pile) is added to the figures.

### Test results of C-series

The test piles with root part (from C-60 to C-120) show larger pile end resistances ( $R$ ) than that of the standard pile (SP) because of enlarged-diameter effect. And the test piles of C-60 to C-120 show almost the same resistance values until 3.5 mm of displacement. However, after that, the increase rates of the resistance are reduced, and the resistance values decrease suddenly. Then, it is surmised that the destruction of the root hardening part has arisen. The magnitude order of the maximum resistance ( $R$ ) is C-60 > C-80 > C-100 > C-120, and the smaller the water-plaster ratio, the larger the maximum resistance.

Table 3 show the relationship between water-plaster ratio (W/P) and compressive strength. Fig. 7 shows the relationship between the water-

Table 3 Relationship between water-plaster ratio and compressive strength

Water-Plaster ratio W/P (%)	Compressive strength (N/mm <sup>2</sup> )
60	5.25
80	4.43
100	2.79
120	1.67

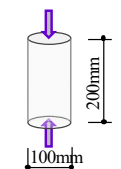
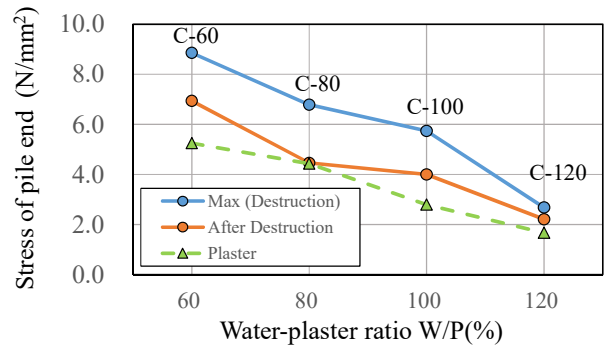



Fig. 7 Relationship between water-plaster ratio and destruction stress of pile end (C-series)

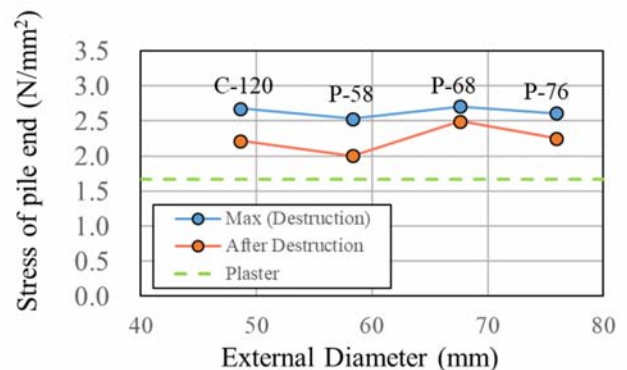


Fig. 8 Relationship between external diameter of the end plate and destruction stress of pile end (P-series)

plaster ratio and the stress of the pile end before and after destruction of the root part. The stress is the quotient of the end resistance divided by the pile tip area, and plaster compressive strength is added to the figure. The pile end stresses at the destruction (maximum values) are approximately 1.5 times large as the compressive strengths of the plaster. And even after the destruction, the pile end stresses do not show the smaller values than the plaster's strengths. This phenomenon is presumed to be due to side reaction stress around the pile tip.

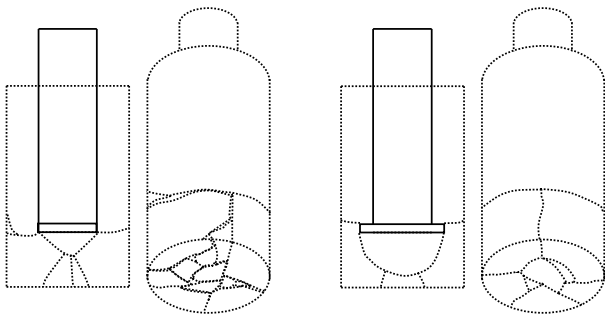
### Test results of P-series

In the P-series, the R value of P-58 (the diameter of the end disk is  $D_e = 58.3$  mm) is as the almost same as the C-120's. However, the R values of P-68 and P-76 ( $D_e = 67.6$  mm and  $75.9$  mm) are larger than that of the C-120's, and the larger the diameter, the larger the pile end resistance. Furthermore, similar to the C-series, the tip resistance has decreased after the maximum load, but the rate of decrease is relatively small.

Fig. 8 shows relationship between the external diameter ( $D_e$ ) of the end disk plate and the stress of the pile end before and after destruction of the root part. The pile end stresses of C-series at the root breakage are almost the same value of  $2.5$  N/mm<sup>2</sup>, and is also same as that of C-120's. The end resistance of a pile with the end disk plate does not decrease greatly even after the root breakage because the pile end has a large effective area. And the pile with the end disk plate will exhibit sufficient end resistance even if the stiffness of the root hardening part would be insufficient.

### Destruction shape of root part

After the loading test, the test pile is excavated and the destruction condition of the root part is observed. Fig. 9 shows the destruction shape of C-60 (W/P = 60 %, closed end pile) and P-68 (W/P = 120 %, pile with end disk plate). Both specimens exhibit a similar destructive shape. The both roots part. Cracks are observed in a wedge shape just below the pile tip, and the occurrence of the split failure is presumed in surrounding area of the wedge.



(a) C-60, W/P=60% (Closed end pile) (b) P-68, W/P=120% (Pile with end disk plate)  
Fig. 9 Destruction condition of root part

## SIMPLIFIED CALCULATION METHOD

### Calculation model

It was understood that the end resistance of pile with root part was larger than that of the pile without root even if the root strength was weak. Furthermore, the end resistance of pile with root did not become smaller than that without root even after the root part broke.

Therefore, we propose a simple calculation model as shown in fig. 10. This model assumes two nonlinear springs, one spring handles the resistance of the pile body ( $P_p$ ), and another spring responds for the

resistance of surrounding the body ( $P_r$ ). And the pile end resistance ( $R$ ) is given as the sum of these as follows;

$$R = P_p + P_r \quad (1)$$

The load-displacement relationship ( $q$ - $y$  curve) of the each spring is set as follows.

### Relationship between pile end stress and displacement

The stress of pile end ( $q$ ) and displacement ( $y$ ) are defined by the reference displacement ( $0.1D$ ) and the stress of  $q_{max}$ , which is the stress at the reference displacement ( $0.1D$ ).

$$q_{max} = \alpha N_t \quad (2)$$

where,  $\alpha$  is the bearing capacity factor and  $N_t$  is the N-value at pile end. Then, a trilinear skeleton curve is assumed as shown in fig. 10. The function of each line is as follows;

$$\text{1st line: } \frac{q}{q_{max}} = \frac{y}{6D} \quad \left(\frac{y}{D} < 0.02\right) \quad (3)$$

$$\text{2nd line: } \frac{q}{q_{max}} = \frac{y}{12D} + \frac{1}{6} \quad \left(0.02 \leq \frac{y}{D} < 0.1\right) \quad (4)$$

$$\text{3rd line: } \frac{q}{q_{max}} = \frac{y}{30D} + \frac{2}{3} \quad \left(0.1 \leq \frac{y}{D}\right) \quad (5)$$

### Pile end resistance force

The resistance force  $P_p$  and  $P_r$  are calculated as follows;

$$P_p = \alpha N_t A_p, \quad P_r = \alpha N_t A_r \quad (6)$$

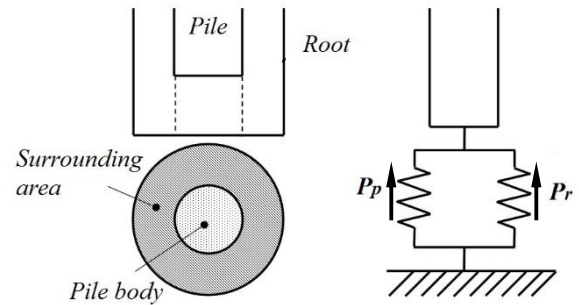


Fig. 10 Calculation Model

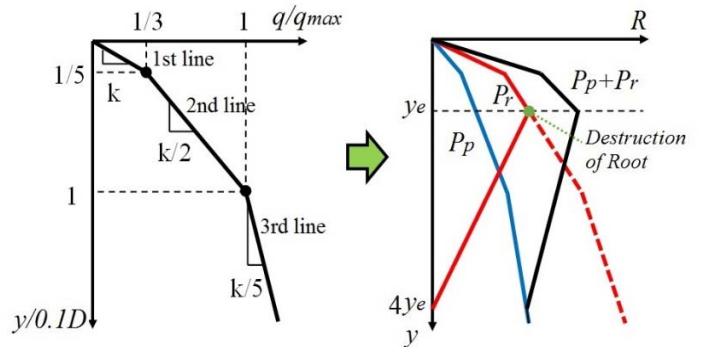


Fig. 11 Pile end resistance ( $R$ - $y$  curve)

where,  $A_p$  and  $A_r$  are the areas of the body portion and the surrounding portion, respectively. Moreover, as shown in fig. 11, it is assumed that the surrounding spring force  $P_r$  gradually decreases until 4 times of the displacement of  $y_e$  ( $y_e$ : breakage displacement) after the root break. In above manner, the relationship between pile end resistance force and displacement, i.e.  $P_p$ - $y$  curve and  $P_r$ - $y$  curve are determined.

### Comparison between test and calculation results

To examine the validity of the calculation method, comparisons with the laboratory test results are carried out. In case of the test without root (SP), of which depth of embedment is  $H=250$  mm, the N-value at the pile end is set as  $N_t=2$ , and in other cases, that is, the test with the root ( $H=300$  mm) are set as  $N_t=3$  (see fig. 3). The bearing capacity factor ( $\alpha$ ) which depends on the construction method and end shape of pile is set as  $\alpha=600$  (kN/m<sup>2</sup>) in C-series, and is set as  $\alpha=500$  (kN/m<sup>2</sup>) in P-series.

The destruction stress of the root part applies as 1.5 times of compressive strength of the plaster (see figs. 7 and 8).

Figs 12 and 13 show a comparison between laboratory test and calculation results. The calculated value of the SP-pile is in good agreement with the experimental result. This result shows that the characteristics of the pile body spring ( $P_p$ - $y$  curve) are suitable.

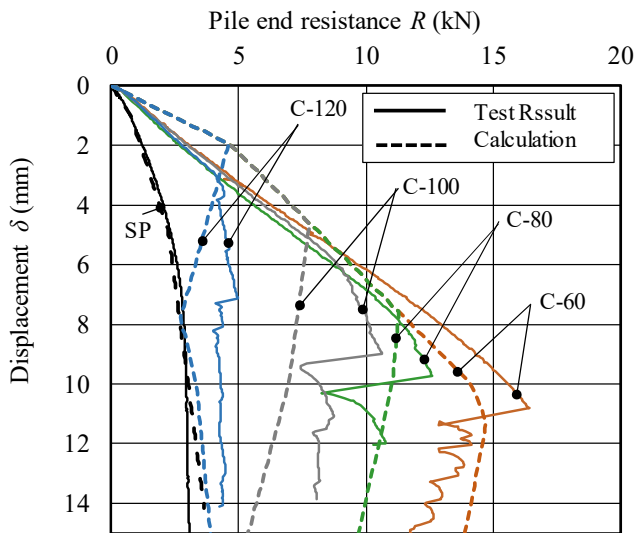


Fig. 12 Comparison between test and calculation results (C-series)

In the C-series, the root destruction load of the calculation and test results shows approximately same value. And after the destruction, the decline of the load is also roughly the same. However, at the phase of the load increasing, the calculation values are larger than the test results. It is presumed that this phenomenon is caused by lack of the stiffness of the root part, and some improvements of the  $P_r$ - $y$  curve will be required.

In the P-series, as same as the C-series, although the calculation values are larger than the test results at the load increasing stage, the calculation results are well simulating the destruction of the root and subsequent transition of the resistance.

This calculation method can be applied to a safer pile design because it

can estimate the relationship between pile tip resistance and displacement considering the destruction of the root part. However, when applying this method to an actual pile, it is necessary to determine the bearing capacity factor ( $\alpha$ ) and the destruction strength of the root taking into consideration the characteristics of the supporting layer and the scale effect.

### CONCLUSION

The pile end resistance of the bored pile is affected by the strength of the root part, and when the root part breaks, the resistance decreases suddenly. The pile which has a large disk plate onto the tip, does not suffer a large load reduction even if the root is destroyed. The simplified calculation method was proposed which can consider the behavior of the destruction of the root part. In this method, the load-displacement relationship can be estimated from only the N-value and the bearing capacity factor. The calculation method was comparatively in good agreement with the laboratory experiment results by applying the appropriate destruction stress of the root.

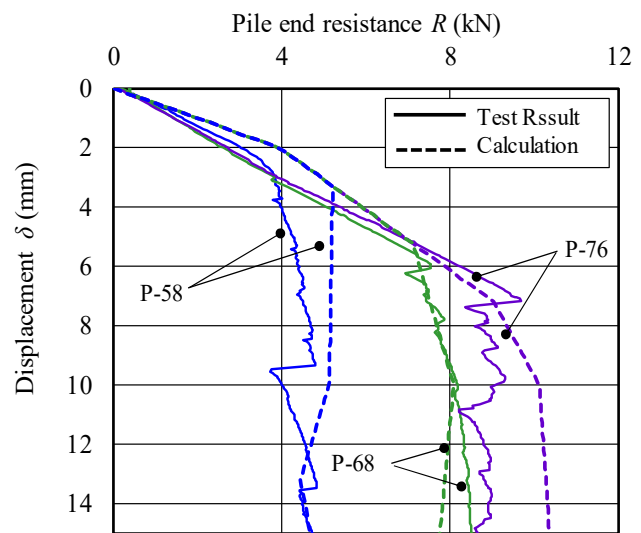


Fig. 13 Comparison between test and calculation results (P-series)

### ACKNOWLEDGEMENTS

Special thanks are due to Mr. S. Matsumoto and S. Miyazaki, graduate students of Nihon University, for their cooperation in the laboratory experiment.

### REFERENCES

- Ishikawa, K, ITO, A and Ogura, H (2012). "Effect of Tip Length and Strength of Enlarged Grouted Base on Bearing Capacity of Straight Pile - Model Test on Enlarged Grouted Base of Bored Precast Pile Part 2 -", *Journal of Structural and Construction Engineering, Architectural Institute of Japan* (in Japanese), 676, 883-889.

- Kiya, Y, Kato, Y and Kuwabara, F (2007). "Model Tests on Vertical Bearing Performance of Enlarged Base of Buried Nodular Piles", *Journal of Structural and Construction Engineering, Architectural Institute of Japan* (in Japanese), 615, 137-143.
- Miyazaki, S, Sato, H and Kanuka, K (2015). "Consideration for End Shape of a Pile for Prebored Pile Construction Method", *Proc 25th International Offshore and Polar Engineering Conference (ISOPE)*, 780-784.
- Sato, H, Kanuka, K and Miyazaki, S (2016a) "Study on End Bearing Capacity of Cement Milk Pile Construction Method for Steel Pile", *AIJ Journal of Technology and Design, Architectural Institute of Japan* (in Japanese), 51, 471-476.
- Sato, H, Kanuka, K and Miyazaki, S (2016b). "Laboratory Experiment for End Bearing Capacity of Pile with Fragile Root Hardening Part", *Proc 26th International Offshore and Polar Engineering Conference (ISOPE)*, 478-482.
- Tsuchiya, T and Kuwabara, F (2012). " A Study on the Compressive Strength of the Base Bulb of Bored Piles Affected by Construction Methods", *AIJ Journal of Technology and Design, Architectural Institute of Japan* (in Japanese), 40, 883-888.
- Ueno, K, Kurachi, S, Ohi, A and Yokoyama, Y (1993). "Shape Effect on Failure Mechanism of Tip Protected Pile", *Proc 28th Japan National Conference on Geotechnical Engineering* (in Japanese), E-4, 1731-1734.